Imaging of the Iron Mountains and Lusatian thrust faults (Czechia) by audiomagnetotellurics, gravity and resistivity surveys

Radek Klanica[1], Petr Tábořík[2], Jakub Stemberk[2]
1) Institute of Geophysics, CAS 2) Institute of Rock Structure and Mechanics, CAS

Motivation

- thrust (reverse) faults are a type of dip-slip faults, where upper block, above the fault plane, moves up and over the lower block
- typical for areas of compression
- thrust faults have shallow dip angle, reverse faults more than 30°

GOAL:

- used combination of shallow geophysical methods with audiomagnetotellurics to image thrust fault architecture and interpret faults evolution

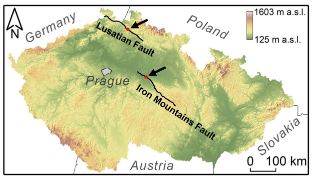

Figure 1. Emplacement of both investigated faults and sites within the area of the Czech Republic.

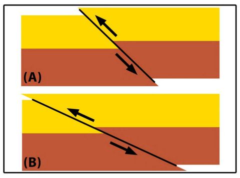

Figure 2. Reverse (A) vs thrust (B) fault.

Investigated sites

- The **Iron Mountains Fault (IMF)** was reactivated as reverse/thrust fault during the Alpine orogeny. It separates paleozoic Iron Mountains Crystalline from the Czech Cretaceous Basin (*Coubal et al., 2019*).

- The **Lusatian Fault (LF)** is prominent product of the Cretaceous to Paleogene thrusting in the Alpine foreland. Its fault plane dips to the N/NE and separates paleozoic Krkonoše-Jizera Crystalline Complex from the Czech Cretaceous Basin. At the locality dips under low to moderate angles (*Coubal et al., 2014*).

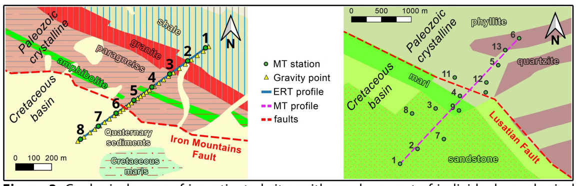

Figure 3. Geological maps of investigated sites with emplacement of individual geophysical methods. Both faults delimit the Czech Cretaceous Basin from adjacent crystalline units.

Methodology

Audiomagnetotellurics:

- registered horizontal components with ADU07e and MFS07e induction coils, part of LF sites with MTU5
- on **IMF** measured 8 stations with spacing of 150 m along profile, 1h recordings with 4096 Hz sampling
- on **LF** measured 13 stations in irregular grid around the fault, 20h recordings with 128 and 4096 Hz sampling
- dimensionality considered by phase tensors (*Caldwell et al., 2004*) - both sites show 3D structures (**Fig. 4**)
- data processed by ProcMT (*Friedrichs, 2021*) using robust stacking technique (**Fig. 5A/5B**)
- data quality poor due to cultural noise - only data up to period 1 s were used for inversions (depths 1-2 km)
- data inverted using 3D code ModEM (*Egbert and Kelbert, 2012*) - **IMF** without topography (**Fig. 8**), **LF** with topography based on adjusted SRTM90 (**Fig. 9**)

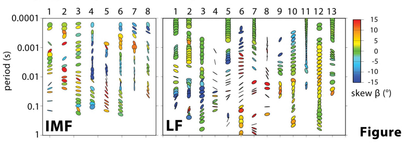

Figure 4. Phase tensors for both sites.

Electrical Resistivity Tomography:

- so far done only on **IMF** site
- 1075 m long profile with 5 m electrode spacing using Wenner-Schlumberger array
- data inverted in Res2DInv (*Loke and Barker, 1996*) with topography based on LiDAR DEM (**Fig. 7**)

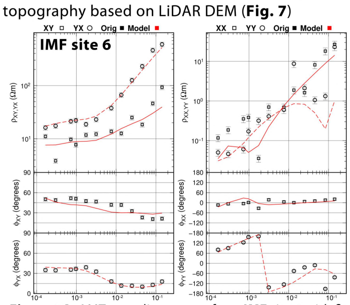

Figure 5A. AMT sounding curves from **IMF** site 6 with fit of final 3D model from ModEM with RMS of 3.68%.

Gravity survey:

- so far done only on **IMF** site, 1100 m long profile with 31 gravity points with spacing 50 m further from the fault and 25 m around the fault
- data corrected for instrumental drift, tidal effects, point elevation and terrain correction, for Bouguer correction was used density of 2.67 kg/m³ (**Fig. 6**)
- data modelled in 2D using GM-SYS (*GM-SYS, 2017*),

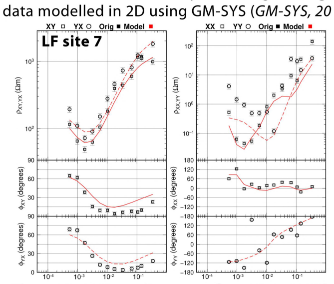

Figure 5B. AMTsounding curves from **LF** site 7 with fit of final 3D model from ModEM with RMS of 2.73%.

Results

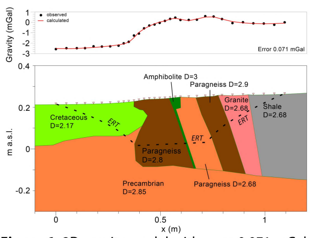

Figure 6. 2D gravity model with error 0.071 mGal (densities in g/cm³) with highlighted ERT section.

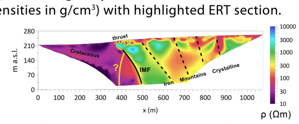

Figure 7. 2D ERT model with RMS 13% shows IMF thrust over the Cretaceous basin. Continuation of IMF into depth has two possibilities (yellow „?“).

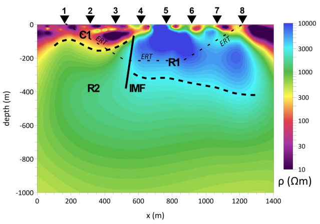

Figure 8. 2D profile from 3D MT model of IMF showing the Cretaceous basin (C1), Iron Mountains Crystalline (R1) and Proterozoic basement (R2) with possible IMF placement.

IMF

Result IMF:

ERT and gravity modelling suggest, that the Iron Mountains Crystalline is only slightly thrusted over younger units. MT model shows inclination of the IMF in greater depth and shows possible emplacement of older fault.

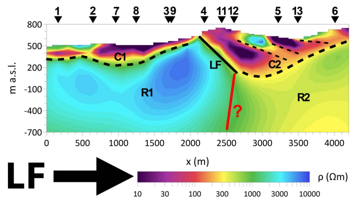

Figure 9. 2D profile from 3D MT model of LF showing the Cretaceous basin (C1), upper Paleozoic Crystalline (C2) and R1/R2 structures related to basement Paleozoic crystalline complexes.

Result LF:

MT model shows inclination of LF largely confirming studies based on geological mapping. In addition, MT suggest possible continuation of LF into depth, when it originally separated Paleozoic blocks in past .

Conclusions

Presented approach shows, that combination of applied geophysical methods with deeper reaching audiomagnetotellurics is beneficial. Whereas, ERT, gravity or shallow seismic methods are able to image faults in their near surface parts (below ca. 200 m); audiomagnetotellurics can supplement these data by deeper information. This combination, applied to thrust/reverse faults, allow to image: (1) thrust itself and possibly evaluate movement on the fault from thrusted part; (2) deeper part of fault originating before the thrusting itself. Subsequent combination of this outcomes with geological information can help to reconstruct geological/faults evolution and areas tectonics.

References

Caldwell T. G., Bibby H. M., Brown C. (2004) The magnetotelluric phase tensor. Geophys. J. Int., 158/2, 457-469.
Coubal, M., Adamovič, J., Málek, J., Prouza, V. (2014) Architecture of thrust faults with alongstrike variations in fault-plane dip: anatomy of the Lusatian Fault, Bohemian Massif. Journal of Geosciences 59, 183-208.
Coubal, M., Zelenka, P., Stemberk, J. (2019) Record of Alpine tectonic activity of the Železné hory Fault expressed by brittle deformation within its southeastern segment. Geoscience Research Reports 52, 141-146.
Egbert, G.D., Kelbert, A. (2012) Computational recipes for electromagnetic inverse problems. Geophys. J. Int. 189, 251–267.
Friedrichs B. (2021) MT Processing code. https://manuals.geo-metronix.de/en/procmt/procmt.html.
GM-SYS Modelling (2017) Gravity modelling code. http://www.geosoft.com/products/gm-sys
Loke, M. H., Barker, R. D. (1996) Rapid least-squares inversion of apparent resistivity pseudosections by a quasi-Newton method. Geophysical Prospecting, 44, 131–152.

Acknowledgement
Thanks Y. Avram and G.J.Hill for providing phoenix instruments and measurements on LF site.